Studies of Unoccupied Orbitals of BF_3 and BCl_3 by Electron Transmission Spectroscopy and Multiple Scattering Xα Calculations

J. A. TOSSELL AND J. H. MOORE

Department of Chemistry, University of Maryland, College Park, Maryland 20742, U.S.A.

J. K. OLTHOFF

Department of Physics, University of Maryland, College Park, Maryland 20742, U.S.A.

Abstract

Electron transmission spectroscopy (ETS) and bound-state and continuum multiple-scattering Xα (MS-Xα) calculations are employed to characterize the unoccupied a_2'', a_1' and e' orbitals of BF_3 and BCl_3. The a_2'' orbital of BF_3, which produces a peak about 7 eV below threshold in the x-ray absorption spectrum (XAS), generates a scattering resonance at 3.5 eV in ETS. Similarly, the e' orbital that lies about 2 eV above threshold in XAS occurs about 13–16 eV above threshold in ETS. Dissociation of F^- from BF_3 due to electron attachment is attributed to a core-excited shape resonance involving an $e'' \rightarrow a_2''$ excitation and electron capture into the a_2'' orbital. In BCl_3 all the unoccupied orbitals lie at lower energy than in BF_3 and are closely spaced, making definitive spectral assignments difficult. Both Hartree–Fock (HF) and MS-Xα methods apparently underestimate the stability of the unoccupied e' orbital of BCl_3. Vibronic coupling due to out-of-plane bending may significantly affect the spectral intensities. Feshbach resonances are observed for BCl_3 at energies close to those observed in the vacuum-UV absorption spectrum. The lower energies of the unoccupied orbitals of BCl_3 are consistent with their stronger bonding to nucleophiles.

Introduction

It is well known that the boron trihalides are strong Lewis acids [1]. However, for BF_3 the adiabatic electron affinity is negative [2], and it is known that the adiabatic electron affinity is considerably more positive than the vertical electron affinity due to large, stabilizing, out-of-plane geometric distortion in the anion [3]. Only orbitals with negative vertical electron affinities are observable by electron transmission spectroscopy (ETS). Although there has been no previous direct observation of electron capture into unoccupied orbitals of the boron halides, there are both experimental measurements and theoretical calculations that relate to the energies and other properties of these orbitals. For example, a resonance presumably associated with temporary anion formation has been observed in the electron impact vibrational excitation of BF_3 [4]. Furthermore, some information is available on UV and x-ray absorption [5, 6] that involves electron excitation into the unoccupied orbitals. Theoretical studies using HF-based Stieltjies imaging [6] and equivalent ionic-core virtual orbital [6] methods, as well as multiple-scattering (MS) Xα techniques [7] have been employed in the interpretation of the x-ray absorption spectra. In the present work we have used

ETS to determine the energies of temporary negative-ion states in BF_3 and BCl_3 that arise from electron capture into low-lying unfilled molecular orbitals. In addition, we have undertaken MS-Xα calculations, using the Slater transition-state concept [8] to relate the electron transmission, x-ray, and UV absorption results.

Experimental Method

The electron transmission experiment involves the measurement of the transparency of a gas to an electron beam as a function of energy. The transparency depends in an inverse fashion upon the electron-scattering cross section. Temporary negative-ion formation occurs with large cross section only over a narrow energy range. Treated as a scattering process, such a temporary ion appears as a phase change of π in the scattering electron wave function and as a maximum in the electron-scattering cross section. We shall refer to this process, as well as the corresponding feature in the transmission-vs.-energy spectrum, as a "resonance."

The electron spectrometer consists of an electron source followed by an electron monochromator, a gas cell, and an electron collector [9]. In practice, the first derivative of the transmitted current as a function of energy is recorded, since the derivative is sensitive to the abrupt change in transmitted current associated with a resonance [10]. The energy associated with a resonance is known as an "attachment energy" (AE) and, with respect to the derivative spectrum, is defined as the point vertically midway between the minimum and maximum that characterize the resonance. For the present purposes an attachment energy may be identified with the negative of the corresponding vertical electron affinity [11]. The chief limitation is that ETS gives only the energy associated with unstable negative ions. That is, only negative electron affinities can be obtained with ETS. A time-of-flight mass spectrometer has recently been appended to the ETS apparatus to monitor anions from dissociative attachment. Thus, for example, we observe anions from the process $e^- + BX_3 \rightarrow BX_2 + X^-$.

Computational Method

The continuum MS-Xα method has been previously described [12, 13]. We have applied this method using transition state potentials to the series $(C, Si)X_4$, $X = H, F,$ Cl [14]. In the present work we use D_{3h} symmetry for BF_3 and BCl_3 with experimental bond distances of 1.307 Å and 1.742 Å, respectively [15]. Atomic sphere radii were chosen according to the prescription of Norman [16] with approximately 20% overlap [17]. Alpha values were obtained in the usual way by using the tabulations of Schwarz [18]. For the calculations of elastic electron-scattering cross-section, experimental dipole polarizabilities [19] were used, and the polarization potential was assumed to have the functional form $-\alpha/r^4$. All calculations were carried out in a spin-restricted formalism. Maximum azimuthal quantum numbers were 4 on the outer sphere and on the central atom, and 2 on the halogens.

Results

The ground state MS-Xα orbital energy diagram of BCl_3 is shown in Figure 1. The $1a_1'$ and $1e'$ orbitals are predominantly Cl3s in character, the $2a_1'$ and $2e'$ are B2s-Cl3p
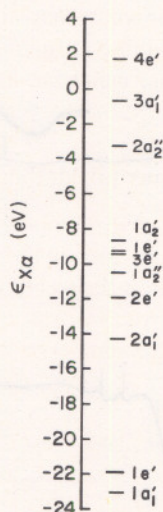
Figure 1.   Ground state MS-Xα orbital eigenvalues for BCl$_3$ (energies in eV; the 1a$_2'$ orbital is the HOMO).

and B3p-Cl3p σ bonding, the orbitals from 1a$_2''$ to the HOMO 1a$_2'$ are predominantly Cl3p nonbonding, the 2a$_2''$ LUMO is B2p-Cl3p π^*, and the 3a$_1'$ and 4e$'$ are B2p-Cl3p σ^* orbitals. The BF$_3$ eigenvalue spectrum is similar, except that all the empty a$_1'$ orbitals are higher in energy and more diffuse than for BCl$_3$. We shall employ the same orbital numbering scheme for BF$_3$. Based on this simple orbital model, we would expect that transient negative ions could arise by capture of electrons into the 2a$_2''$, 3a$_1'$, or 4e$'$ orbitals, although the stability of the 2a$_2''$ in BCl$_3$ is great enough that anions formed by its occupation could be quite close to threshold. In Figure 2 we present the derivative ETS spectrum for BF$_3$ and BCl$_3$. Figure 3 is a correlation diagram showing the attachment energies for the two molecules and giving the most probable orbital assignments. Continuum MS-Xα elastic scattering cross sections for BF$_3$ and BCl$_3$ are shown in Figure 4. For both molecules the potential used in the continuum MS-Xα calculation was obtained self-consistently with 0.5 electrons in the 2a$_2''$ orbital. Previous experience suggests that cross sections near threshold in the totally symmetric channel are exaggerated by the method [20] so that the threshold behavior shown in Figure 4 is certainly suspect.

The electron scattering between 0.1 and 0.8 eV in BF$_3$ is due to vibrational excitation of neutral BF$_3$. An expanded spectrum of this region is shown in Figure 5. This process has been observed previously for CF$_4$ [21]. The spacing between the vibrational features alternates between two values of approximately 0.08 eV and 0.10 eV. Four modes of vibrational excitation are possible for neutral BF$_3$ [22]. The vibrational energies of the different modes are $\Delta E(\nu_1) = 0.110$ eV, $\Delta E(\nu_2) = 0.0085$ eV, $\Delta E(\nu_3) = 0.180$ eV, and $\Delta E(\nu_4) = 0.060$ eV. The spacing of the vibrational features in Figure 5 thus indicates that ν_3 (the asymmetric stretch mode) and ν_2 (the umbrella mode) are excited. The first feature near 0.18 eV corresponds to $\nu_3 = 1$ and $\nu_2 = 0$.

Figure 2.   Derivative electron transmission spectra of BF_3 and BCl_3. The spike at 0 eV in each spectrum is simply the derivative of the abrupt turning on of current at threshold. The spike in the BF_3 spectrum is characteristic of the resolution of the experiment. The broadening of the spike for BCl_3 implies an attachment process at threshold. For BF_3 the insert shows an expanded version of the region from 10–16 eV, showing a weak but reproducible resonance.
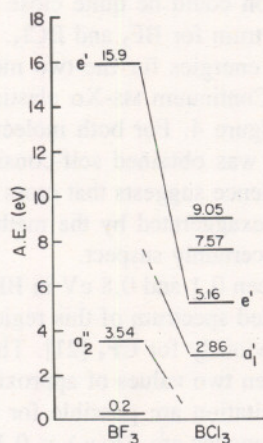

Figure 3.   Correlation diagram giving the attachment energies (AE) for BF_3 and BCl_3. Probable assignments for the orbitals responsible for the observed anion states are also given.

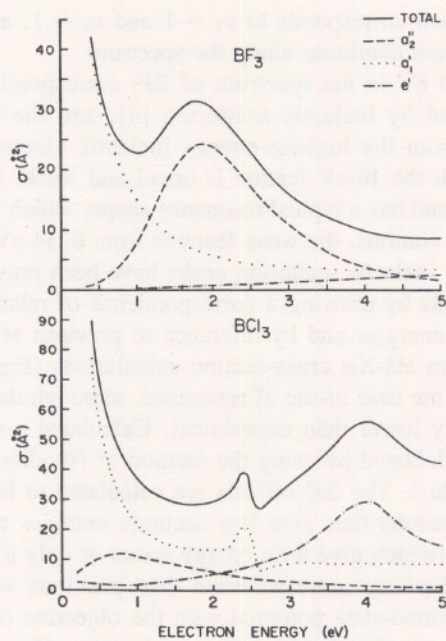Figure 4.   Continuum MS-Xα elastic electron-scattering cross sections for BF$_3$ and BCl$_3$: total, - - - a$_2''$ symmetry, · · · · a$_1'$ symmetry, - · - e symmetry.
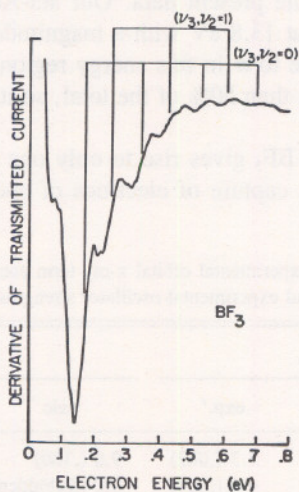

Figure 5.   Derivative electron transmission spectrum of BF$_3$ expanded to show vibrational excitation near threshold.

The second feature then corresponds to $\nu_3 = 1$ and $\nu_2 = 1$, and the next to $\nu_3 = 2$ and $\nu_2 = 0$. This pattern continues along the spectrum.

The feature at 3.54 eV in the spectrum of BF_3 corresponds fairly closely to the 3.8-eV peak observed by inelastic scattering [4], and the broad feature around 16.9 eV is not far from the highest-energy inelastic electron-scattering peak at 13.7 eV [4]. Although the 16-eV feature is broad and weak, it is reproducible over the course of months and has a typical resonance shape, which is clearly shown in the insert in Figure 2. By contrast, the weak features from 6–14 eV are not reproducible. The 3.8- and 13.7-eV inelastic scattering peaks have been previously assigned [4] to the $2a_2''$ and $4e'$ orbitals by drawing a correspondence of relative electron scattering and x-ray absorption energies and by reference to previous MS-Xα calculations [7]. The present continuum MS-Xα cross-section calculations (Fig. 4) certainly support this interpretation for the case of the a_2'' resonance, although the calculated resonance energy is considerably lower than experiment. Calculated x-ray term energies and oscillator strengths calculated by using the method of Noodleman [23] are given for BF_3 and BCl_3 in Table I. The $2a_2''$ orbitals are calculated to be too stable by 1.3 to 1.6 eV. The present results thus give less accurate energies than the Hartree–Fock approaches of Ref. 6 (which give term energy errors of only a few tenths of an electronvolt), although they are more accurate than previous MS-Xα results [7] that employed only the ground-state potential with the objective of obtaining a comprehensive picture of the near threshold continuum structure. If we correct the calculated a_2'' resonance energy of 1.9 eV in BF_3 by the difference of 1.1 eV between calculated and experimental x-ray term energies, we project the a_2'' resonance to be about 3.0 eV, in reasonable agreement with experiment. Assuming that the $4e'$ XAS term energy and the e' ETS resonance energy differ by the same amount as for the $2a_2''$ (~ 10.8 eV) leads to a projection of 13.1 eV for the e' resonance, in reasonable agreement with Ref. 4 and the present data. Our MS-Xα cross-section calculations also give a broad maximum at 13.8 eV with a magnitude of 16.0 Å [2]. Although a number of channels contribute to σ in this energy region, only the e' shows a maximum, and it contributes more than 50% of the total, so it is reasonable to call this an e' resonance.

Dissociative attachment to BF_3 gives rise to only one peak in the mass spectrum. As previously observed [24], capture of electrons of about 11.3 eV energy leads to

TABLE I.   Calculated and experimental orbital x-ray term energies (in eV) for BF_3 and BCl_3 (calculated and experimental oscillator strengths in parentheses).

	BF_3		BCl_3	
	calc.	exp.[a]	calc.	exp.[a]
$2a_2''$	8.4 (.105)	7.3 (.082)	9.0 (.100)	7.4 (.022)
$3a_1'$	5.1 (forbidden)	4.6 (.004)	6.0 (forbidden)	3.7 (.0036)
$4e'$	−1.8 (.081)	−2.3 (.195)	1.5 (.023)	2.9 (.043)

[a]Ref. 6.

the production of F$^-$. This peak corresponds to the second peak observed by Tronc et al. [4] in the vibrational excitation spectrum of BF$_3$. This ion peak and the structure in the vibrational excitation spectrum are not well understood because no corresponding feature appears in the electron transmission or photoabsorption spectrum. Possibly this structure is the result of a weak, repulsive resonance or core-excited shape resonance. The lowest energy resonance of this type is expected to correspond to the configuration $(1e'')^{-1}(2a_2'')^2$ arising from a dipole allowed excitation $1e'' \rightarrow 2a_2''$ and the capture of an electron into $2a_2''$. Our MS-Xα calculations give 12.3 eV for the resonance and 11.6 eV for the $1e'' \rightarrow 2a_2''$ excitation energy, leading to classification of the resonance as a core-excited shape resonance. Unfortunately, the only data on the vacuum-UV absorption spectrum of BF$_3$ indicate that there are no singlet absorption bands below 10.5 eV [25], although a triplet absorption may occur at about 8 eV [26]. The 11.3-eV feature is thus energetically consistent with a core-excited shape resonance of the type suggested, but we presently have no way to calculate the intensity of such a feature and no direct experimental correspondence with the UV spectrum.

The ETS spectrum of BCl$_3$ is considerably more difficult to assign. Although the x-ray term energies of the $2a_2''$ orbitals of BF$_3$ and BCl$_3$ are very similar, direct calculation of the vertical AE's using the transition-state approach gives values of 1.6 eV for BF$_3$ and about 0.0 eV for BCl$_3$. This substantial difference arises from the larger size of BCl$_3$, which reduces the magnitude of the $2a_2''$ orbital self-repulsion. If we assume that the underestimation of the $2a_2''$ resonance energy in BCl$_3$ is similar to that in BF$_3$, we would project an $2a_2''$ resonance at about 1.9 eV, but the lowest energy ETS peak occurs at 2.9 eV. The calculated cross sections give only a very weak a_2'' maximum at low energy. The calculations do, however, indicate maxima in the a_1' and e' channels. The a_1' maximum is somewhat unexpected since no such feature occurs in BF$_3$, but a transition-state calculation of the BCl$_3$ $3a_1'$ vertical AE indeed gives a value of 1.2 eV and a localization of about 15% of the electron density within the B atomic sphere. The e' maximum near 4.0 eV is at lower energy than would be expected from the calculated XAS energies in Table I. Although the total cross section is smoothly decreasing from 5.0 to 9.0 eV, above 9.0 eV there is a very slow increase in cross section, leading to a flat maximum at 10.8 eV, with the main contribution being from the e' channel. The complexity of the calculated cross section and the lack of quantitative correspondence with experiment make interpretation difficult.

Similar difficulties appear in the interpretation of the x-ray [6] and UV [25] absorption spectra of BCl$_3$. Although both MS-Xα (Table I) and HF methods give reasonable B1s XAS term energies and intensities for BF$_3$, both methods have problems with the apparent $4e'$ feature in the spectrum of BCl$_3$, giving term energies and relative oscillator strengths that are too small. These discrepancies may arise either from a poor description of the $4e'$ orbital or from vibronically allowed intensity to the $3a_1'$ orbital, which is quite localized in BCl$_3$ as we have indicated. It has been argued that vibrationally excited BX$_3$ molecules will be nonplanar with C$_{3v}$ symmetry, so that the B1s(a_1') $\rightarrow 3a_1'$ transition is allowed [6]. Since the frequency of the out-of-plane a_2'' vibration of BCl$_3$ is one-third smaller than that of BF$_3$ [27], we expect such vibronic coupling effects to be larger in BCl$_3$.

In the same way the MS-Xα calculations give intensities that are too small for the features attributed to 4e$'$ final states in the vacuum-UV spectrum. The spectrum of Planckaert et al. [25] shows maxima at 7.2 and 9.0 eV and a shoulder at 8.3–8.6 eV. A sharp rise in absorption also occurs around 10.5 eV, suggesting another maximum beyond the limit of the study. MS-Xα calculations give two intense transitions: 1e$''$ $\rightarrow$ 2a$_2''$ at 6.3 eV, with $f = 0.195$, and 2a$_1'$ $\rightarrow$ 2a$_2''$ at 11.1 eV, $f = 0.154$. All the intermediate energy transitions allowed in D$_{3h}$ symmetry that involve 3a$_1'$ and 4e$'$ final states have oscillator strengths below 0.01, although their energies fall in the right range. It is conceivable that vibronic effects may also contribute to the intensity in this spectral region.

Our analysis of the UV spectrum of BCl$_3$ does suggest an interpretation of the features observed in the ETS at 7.6 and 9.05 eV. The closeness of these energies to the UV absorption energies of 7.2 and 9.0 eV suggests that they are core-excited shape resonances. MS-Xα calculations give 6.4 eV for the energy of the $(1e'')^{-1}$-$(2a_2'')^2$ state, but this energy may be underestimated just as the x-ray term energy of the 2a$_2''$ orbital is underestimated.

It should be noted that the present MS-Xα calculations give values for orbital ionization potentials accurate to within about 1 eV for the 2a$_1'$-1a$_2'$ orbitals, similar to that obtained from previous studies [28]. The errors in the description of the 2a$_2''$-4e$'$ orbitals are apparently somewhat larger, perhaps due to their larger concentration of electron density in the interatomic region. In addition, ETS resonance energies are very small, so that modest absolute errors are large percentage errors.

Conclusion

The electron transmission spectrum of BF$_3$ shows resonances corresponding to the 2a$_2''$ and 4e$'$ orbitals previously studied by XAS. In addition, a peak in the F$^-$ dissociative attachment spectrum corresponds to a core-excited shape resonance probably involving a $(1e'')^{-1}(2a_2'')^2$ configuration. For BCl$_3$ lower resonance energies are obtained for the 2a$_2''$, 3a$_1'$, and 4e$'$ orbitals, and the ETS shows two low-energy resonances and evidence for an electron capture process at threshold. Both HF and MS-Xα methods appear to underestimate the stability and degree of localization of the 4e$'$ orbital of BCl$_3$, and this underestimation appears in both the x-ray and UV regions of the absorption spectra.

Previous MS-Xα studies have shown a strong dependence of photoionization intensity and electron-scattering cross section upon detailed geometry from some molecules, e.g., CO$_2$ [29] and CF$_4$ [14], although comparison with HF results for CO$_2$ [30] suggests that the MS-Xα distance effects may be exaggerated. The small energy difference of the resonant channels in BCl$_3$ and its low vibrational frequencies suggest the need for further studies at different geometries. We must also systematically explore the use of different transition-state potentials, i.e., those generated by the half-occupation of orbitals other than the 2a$_2''$.

The increase in BX$_3$-donor interaction from BF$_3$ to BCl$_3$, seen e.g., in the B—N bond lengths and stretching force constants of X$_3$B—NCCH$_3$ adducts [31], may be partially related to the greater stability of the 2a$_2''$ orbital in BCl$_3$. Within the context

of the perturbation theory of chemical reactivity [32] a stabilization of the $2a_2''$ orbital should increase the strength of its stabilizing interaction with nucleophiles. It also appears that for BCl$_3$ the $3a_1'$ orbital and perhaps the $4e'$ are also low enough in energy to accept electron density from a nucleophile. If the $4e'$ is active in this respect, one would expect that its relative heat-of-adduct formation would be larger for π-donor adducts, such as CO, that have the proper symmetry to interact with the $4e'$. Studies on the BH$_3$—CO and BF$_3$—CO donor acceptor complexes using Morokuma's energy decomposition analysis [33] indicate a larger charge transfer component to the bonding in BF$_3$—CO, due to a lower energy for the empty a_2'' orbital. A similar analysis of BCl$_3$—CO would be interesting, particularly if a separation of the charge transfer contributions to the $2a_2''$, $3a_1'$, and $4e''$ orbitals could be made.

Acknowledgments

Bibliography

[1] T. D. Coyle and F. G. A. Stone, in *Progress in Boron Chemistry*, H. Steinberg and A. L. McCloskey, Eds., (MacMillan, New York, 1964), Vol. 1.

[2] E. W. Rothe, B. P. Mathur, and G. P. Reck, Inorg. Chem. **19**, 829 (1980).

[3] S. P. So, J. Chem. Phys. **67**, 2929 (1977).

[4] M. Tronc, L. Malagat, R. Aria, and Y. LeCoat, J. Phys. B **15**, L253 (1982).

[5] V. A. Fomichev, Sov. Phys. Solid State **9**, 2496 (1968).

[6] E. Ishiguro, S. Iwata, Y. Suzki, A. Mikuni, and T. Sasaki, J. Phys. B **15**, 1841 (1982). W. H. E. Schwarz, L. Mensching, K. Hallmeier, and R. Szargan, Chem. Phys. **82**, 57 (1983).

[7] J. R. Swanson, D. Dill, and J. L. Dehmer, J. Chem. Phys. **75**, 619 (1981).

[8] J. C. Slater, Adv. Quantum Chem. **6**, 1 (1972).

[9] (a) A. Stamatovic and G. J. Schulz, Rev. Sci. Instrum. **41**, 423 (1970). (b) M. R. McMillian and J. H. Moore, Rev. Sci. Instrum. **51**, 944 (1980).

[10] L. Sanche and G. Schulz, J. Phys. Rev. **45**, 1672 (1972).

[11] For a discussion of AE's vs. EA's as well as calibration of the ETS spectrum, see J. C. Giordan, M. R. McMillan, J. H. Moore, and S. E. Staley, J. Am. Chem. Soc. **102**, 4740 (1980).

[12] D. Dill and J. L. Dehmer, J. Chem. Phys. **61**, 692 (1974).

[13] J. W. Davenport, W. Ho, and J. R. Schrieffer, Phys. Rev. B **17**, 3115 (1978).

[14] J. A. Tossell and J. W. Davenport, J. Chem. Phys. **80**, 813 (1984).

[15] J. H. Callomon, E. Hirota, K. Kuchitsu, W. J. Lafferty, A. G. Maki, and C. S. Pole, in Landolt-Börnstein, *Numerical Data and Functional Relationships in Science and Technology, New Series, Group II Atomic and Molecular Physics*, K. H. Hellwege and A. M. Hellwege, Eds. (Springer, New York, 1976), Vol. 7.

[16] J. G. Norman, J. Chem. Phys. **61**, 4630 (1974).

[17] N. R. Rösch, W. G. Klemperer, and K. H. Johnson, Chem. Phys. Lett. **23**, 149 (1973).

[18] K. Schwarz, Phys. Rev. B **5**, 2466 (1972).

[19] N. K. Sanyal, L. Dixit, and A. N. Pandey, Ind. J. Pure Appl. Phys. **10**, 329 (1972).

[20] D. Dill and J. L. Dehmer, Phys. Rev. A **16**, 1423 (1977).

[21] G. J. Verhaart, W. J. Van Der Hart, and H. H. Brongersma, Chem. Phys. **34**, 161 (1978).

[22] G. Herzberg, *Molecular Spectra and Molecular Structure. II. Infrared and Raman Spectra of Polyatomic Molecules* (Van Nostrand, New York, 1945).

[23] L. Noodleman, J. Chem. Phys. **64**, 2343 (1976).

[24] K. A. G. McNeil and J. C. J. Thyne, J. Phys. Chem. **74**, 2257 (1970).

[25] A. A. Planckaert, P. Sauvageau, and C. Sandorfy, Chem. Phys. Lett. **20**, 170 (1973).

[26] H. Maria, J. R. McDonald, and S. P. McGlynn, J. Am. Chem. Soc. **95**, 1050 (1973).

[27] K. Nakamota, *Infrared Spectra of Inorganic and Coordination Compounds, 2nd ed.* (Wiley-Interscience, New York, 1970), p. 97.

[28] H. J. T. Preston, J. J. Kaufman, J. Keller, J. B. Danese, and J. W. D. Connolly, Chem. Phys. Lett. **37**, 55 (1976).

[29] J. R. Swanson, D. Dill, and J. G. Dehmer, J. Phys. B **13**, L231 (1980).

[30] R. R. Lucchese and V. McKoy, Phys. Rev. A **26**, 1992 (1980).

[31] D. F. Shriver and B. Swanson, Inorg. Chem. **10**, 1354 (1971).

[32] G. Klopman, J. Am. Chem. Soc. **90**, 223 (1968).

[33] H. Umeyama and K. Morokuma, J. Am. Chem. Soc. **98**, 7208 (1976).